The Influence of Breaking at the Ocean Surface on Oceanic Radiance and Imaging

W. Kendall Melville
Scripps Institution of Oceanography,
University of California, San Diego
9500 Gilman Drive
La Jolla, CA 92093-0213
phone: (858) 534-0478 fax: (858) 534-7132 email: kmelville@ucsd.edu

Award Number: N00014-06-1-0048

LONG-TERM GOALS

The long-term goals of the work are to measure the influence of surface wave breaking on imaging across the surface and develop measurements and models of breaking statistics as input to the interpretation and modeling of oceanic radiance measurements.

OBJECTIVES

Image transmission across breaking surfaces will be measured in both the laboratory and the field. Field measurements of breaking and breaking statistics will be used to quantify the degradation and recovery of image fidelity by surface and subsurface processes associated with breaking, including surface turbulence and bubble entrainment. The PI will collaborate with other PIs in the use of breaking measurements and models to interpret measurements and develop models of oceanic radiance and through-surface imaging.

APPROACH

The transmission of light across the ocean surface, whether downwelling or upwelling, depends strongly on refraction across the air-sea interface. Models of refractive effects depend on the structure of the surface; ideally, the surface displacement and all its spatial and temporal derivatives. However, measuring the surface and its derivatives at all relevant scales is technically not possible at present as the spatial scales range from millimeters to kilometers, and the temporal scales from milliseconds to hours. The task is simplified if the temporal and spatial scales can be related through the dispersion relationship for linear surface waves, $\sigma = \sigma(k)$, where σ is the radian frequency, and $k = |\mathbf{k}|$ is the magnitude of the wavenumber vector; but this only works if the wave slope, $ak << 1$ (linear waves), whereas more generally $\sigma = \sigma(k; ak)$. The most important departures from the linear assumption occur in the neighborhood of breaking waves of all scales, from long large gravity waves, to the much smaller, but just as steep, gravity-capillary waves. In the context of ocean optics, the fact that breaking occurs near the

Report Documentation Page

Form Approved
OMB No. 0704-0188

1. REPORT DATE	2. REPORT TYPE	3. DATES COVERED
2009		**00-00-2009 to 00-00-2009**

4. TITLE AND SUBTITLE	5a. CONTRACT NUMBER
The Influence of Breaking at the Ocean Surface on Oceanic Radiance and Imaging	5b. GRANT NUMBER
	5c. PROGRAM ELEMENT NUMBER
6. AUTHOR(S)	5d. PROJECT NUMBER
	5e. TASK NUMBER
	5f. WORK UNIT NUMBER
7. PERFORMING ORGANIZATION NAME(S) AND ADDRESS(ES) **University of California San Diego,Scripps Institution of Oceanography,9500 Gilman Drive,La Jolla,CA,92093-0213**	8. PERFORMING ORGANIZATION REPORT NUMBER
9. SPONSORING/MONITORING AGENCY NAME(S) AND ADDRESS(ES)	10. SPONSOR/MONITOR'S ACRONYM(S)
	11. SPONSOR/MONITOR'S REPORT NUMBER(S)

12. DISTRIBUTION/AVAILABILITY STATEMENT
Approved for public release; distribution unlimited

13. SUPPLEMENTARY NOTES

14. ABSTRACT

15. SUBJECT TERMS

16. SECURITY CLASSIFICATION OF:			17. LIMITATION OF ABSTRACT	18. NUMBER OF PAGES	19a. NAME OF RESPONSIBLE PERSON
a. REPORT **unclassified**	b. ABSTRACT **unclassified**	c. THIS PAGE **unclassified**	**Same as Report (SAR)**	**12**	

crests of the larger waves gives combinations of large surface displacements and large slopes, which can lead to significant departures from the simplest horizontal planar-surface assumption that leads to a simple Snell's cone. Breaking also leads to surface turbulence, which does not have a dispersion relationship, and therefore no explicit deterministic relationship between the length and time scales of the surface. At the larger scales, breaking also leads to significant air entrainment and the attenuation and scattering of light by bubbles. For all these reasons, a better understanding of the occurrence (statistics) and scales of breaking in the context of light transmission across the ocean surface, will lead to improved forward and inverse models of the oceanic radiance distribution. Figure 1 shows a schematic of the major components that were to be deployed as part of the RaDyO field deployments off the coast of California in September, 2008, and Hawaii in August- September 2009. The centerpiece of the experiments was the direct measurement of imaging through the surface using a subsurface (above-surface) display to generate test patterns and a color video camera above (below) the surface. Additional and concurrent measurements included surface displacement (at various scales) as well as occurrence of breaking and air entrainment using LIDAR, acoustic techniques, and underwater imagery.

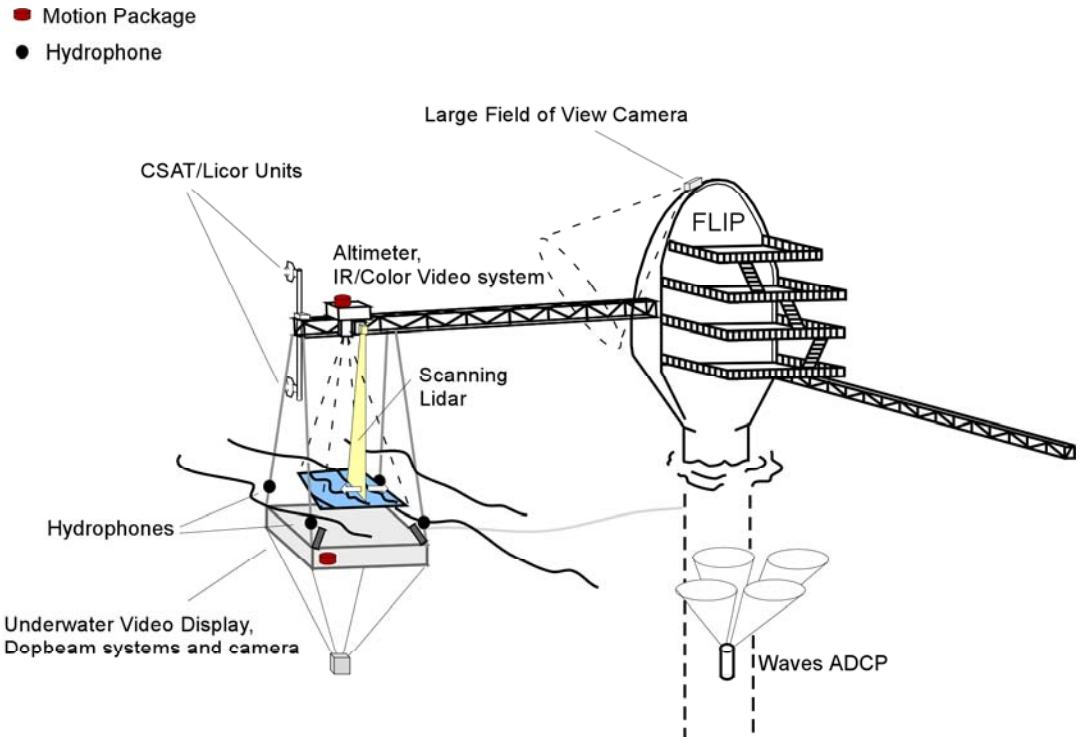

Figure 1: Schematic of the FLIP-based experiments showing the major components of the instrumentation and their deployment.

For imaging through the surface, one of the primary questions concerns the characterization of the fraction of time during which the turbulence and bubbles due to breaking will make any imaging impractical. This requires a statistical description of the probability of breaking over different length and time scales; the characterization of the

time scales between breaking at a point; the distance between breaking events at a particular time, and the time scale for the disturbance (turbulence and bubble clouds) to decay to acceptable levels for imaging.

In a seminal paper, Phillips (1985) introduced, $\Lambda(\vec{c})d\vec{c}$, the average length of breaking fronts traveling with velocities in the range $(\vec{c},\vec{c}+d\vec{c})$. The first moment of the corresponding scalar distribution, $c\Lambda(c)dc$, gives the area per unit area of ocean surface per unit time swept out by breakers traveling in the same speed range. Therefore, $\int_0^\infty c\Lambda(c)dc$ gives the area per unit area per unit time swept out by *all* breakers. If we assume that imaging is impractical during active breaking at a point, this gives a lower estimate of the probability of breaking interfering with imaging during any time interval. Using simple arguments, based on Froude scaling (that the length and time scales are related through the dispersion relationship) it may be shown that the whitecap coverage, the fraction of surface covered by breaking waves, is proportional to the second moment, $\int_0^\infty c^2\Lambda(c)dc$. Similar arguments applied to the depth to which breaking mixes the surface water (and also the small optically-significant bubbles) result in the volume of fluid mixed down by breaking per unit area per unit time being proportional to the third moment, $\int_0^\infty c^3\Lambda(c)dc$. Thus measurements of breaking are fundamental to a determination of the effects of breaking on the transmission of light through the ocean surface and the ability to image through the surface.

WORK COMPLETED

Laboratory Experiments

During 2006-2007 we completed a series of laboratory experiments designed to simulate the effects of wave breaking, entrained air and gravity-capillary waves on the attenuation, scattering and refraction of light transmitted from the atmosphere. The data from those experiments has been compared with field data from the SIO Pier Experiment (see below) measuring the time scales associated with the recovery of through-the-surface images after breaking.

The SIO Pier Experiment

As hosts for the RaDyO SIO pier experiment in January 2008, a significant effort was expended during fall and early winter 2007 to prepare for this three-week experiment. The most visible aspect of this preparation was the design, construction and installation of a new instrument boom on the NW corner of the pier. Along with the original boom on the SW corner of the pier, this provided RaDyO PIs with unprecedented access to incident wind and wave fields from the west. Other aspects of preparation for the pier experiment included the installation of two new lab spaces on the pier, the provision of

trailer/office space just east of the entrance to the pier, the provision of logistical support for the shipping and recovery of equipment, and IT infrastructure for all the PIs.

During the pier experiment we deployed a suite of instruments from the SW boom.. This system included a comprehensive meteorological package including an eddy momentum and (sensible and latent) heat flux package, passive and active IR system for surface imaging and kinematics, a scanning LIDAR for surface wave measurements and an RGB system for imaging transmissions by a submerged programmable LED display. The latter system provided the analogue of the light source in the laboratory studies conducted in 2006-2007.

Santa Barbara Channel Experiment

A: Preparation for the RaDyO Community

As in the SIO Pier Experiment the PI's group assumed much of the infrastructure and logistical responsibility for upgrading FLIP and overseeing the logistics for all the groups using FLIP. This included the design and construction of a starboard boom to accommodate all the instrumentation required. Construction and testing of the boom was funded by a grant from ONR that also covered some of the logistical costs of FLIP's deployment in the Santa Barbara Channel (SBC) Experiment in September, 2008. (N00014-08-1-0383, "Oceanic Radiance and Imaging: FLIP Support for September'08 Experiment") In addition to overseeing the boom construction, Luc Lenain handled much of the logistical interface between the PIs and FLIP for the SBC experiment.

B: Science Program

The Santa Barbara Channel Experiment was conducted in September 2008. Due to the unavailability of a Navy tug for FLIP deployment a smaller commercial tug was used. This was not optimal and it was a difficult FLIP deployment which may have contributed to the port boom being irreparably damaged during its subsequent deployment. We were left with just the starboard and face booms. This limited the boom space for instrument deployment by the PIs and time for intermittent measurements from the booms had to be shared between PIs.

Notwithstanding the setback of having only two booms rather than three, analysis of the data from the experiment has shown it to be a rich data set. Some analysis of the data is shown below.

Hawaii Experiment August-September, 2009

A. Preparation for the RaDyO Community

Following the destruction of the port boom and issues with contamination of some data due to effluent discharges from FLIP during the Santa Barbara Channel Experiment, the PI secured an expansion to N00014-08-1-0383 (reported separately) to cover the design construction and installation of a new port boom and sewage holding tanks for FLIP. As

part of a separate ONR DRI (HiRes), new satellite communications/internet equipment was installed on FLIP and was available for the Hawaii experiment.

B. Science Program

Following weather delays due to Hurricane Hilda, FLIP was towed from Pearl Harbor August 28 at 0800, reaching its deployment site 18-0.0' N 155-30' W August 29 at 1400 from which it subsequently drifted to 17-52.549' N 159-42.413' W over the 17 days of the experiment. It was then towed back to Pearl Harbor, reaching port on September 16 at 1500. Figure 2 shows the deployment of our instrumentation on the port boom during the experiment. This was supplemented with video equipment mounted on the crows nest and in-water instruments for imaging through the surface and for near-surface turbulence and thermal structure measurements (Figure 3) to correlate with the imagery.

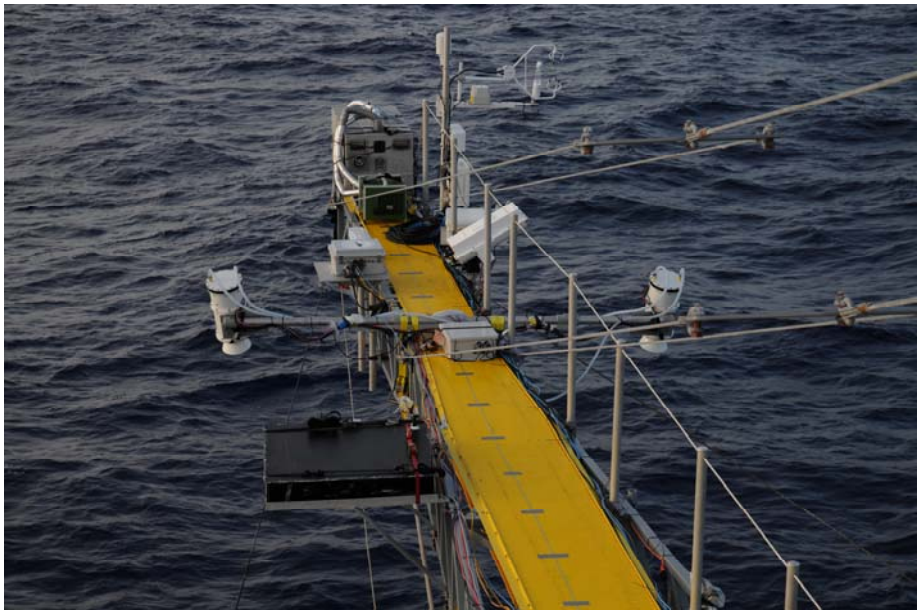

Figure 2: Instrumentation mounted on the port boom in the Hawaii Experiment: light box (foreground); stereo IR imaging system; nadir-looking visible, IR, laser wave gauge, active IR system and met station (end of boom)

RESULTS

Laboratory Experiments

Results from the laboratory experiments have been reported in earlier annual reports.

SIO Pier Experiment

Results from the SIO Pier Experiment were included in the 2008 annual report.
The most important results of the pier experiment were the demonstration of a transition from unbroken to broken surfaces at low wind speeds and its impact on imaging through the surface. The measurements demonstrated that the evolution of the pixel intensity

distribution from bimodal to unimodal to bimodal, as seen in the laboratory following breaking, also occurred in the field. Figure 4 shows the distribution of pixel intensity during a wave breaking event, on January 17th 2008, at 16:37 (local time) in the red band of the RGB camera (the pattern was constituted of red and black stripes at this time).

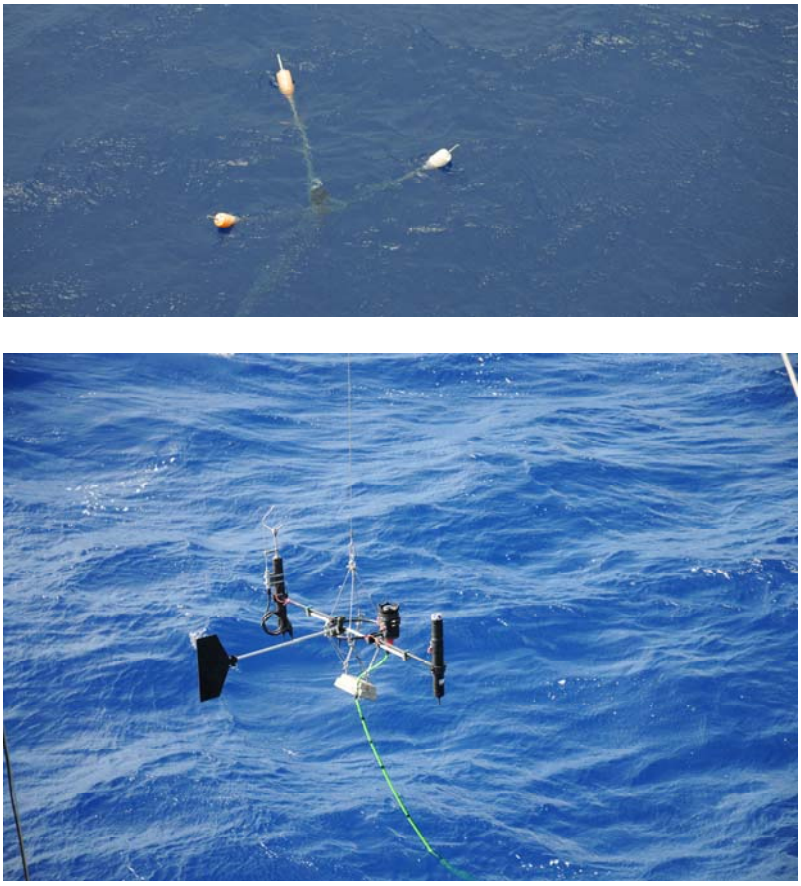

Figure 3: Subsurface processes measurements during Hawaii Experiment (a) upward looking HR Aquadopp mounted on light float, for near-surface turbulence and bubble measurements. (b) Video/Aquadopp/ADV profiler for imaging the light box through the surface and making surface wave, current and turbulent velocity measurements.

The intensity of transmitted light shows the evolution from bimodal to unimodal distributions during breaking, and then a slow recovery to the original bimodal distribution. This is the same qualitative behavior as was seen in the laboratory studies and demonstrates that the duration of image deterioration due to breaking can be quantified. In a practical sense, this is one of the most important metrics of imagery through the surface: the fraction of time the image is degraded by breaking and small scale roughness at the surface.

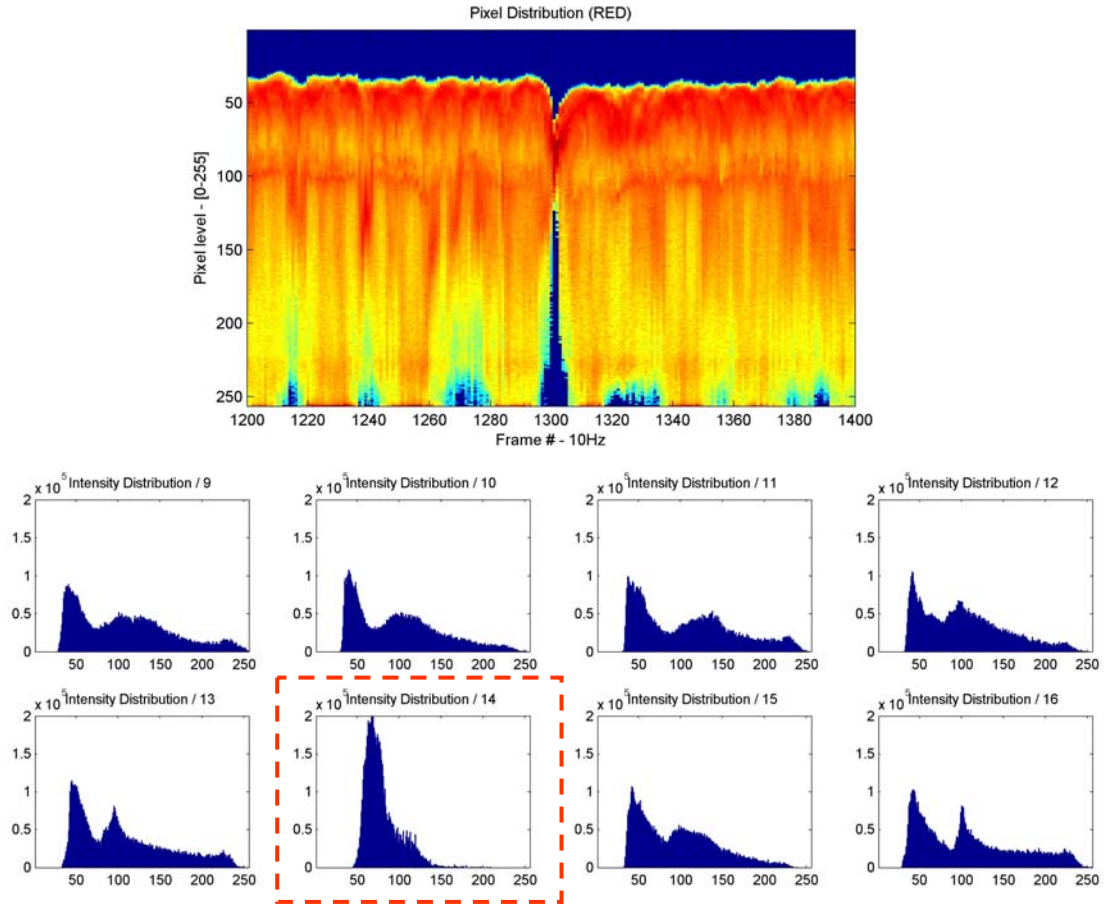

Figure 4: Evolution of the pixel intensity distribution in the red channel going from bimodal to unimodal to bimodal, before during and after a breaking event passes across the surface. This can be compared with qualitatively similar results in the laboratory.

Santa Barbara Channel Experiment

Figure 5 shows a diagram and list of the instrumentation deployed on the port boom and details of some of the instrumentation.

Figure 6 shows spectrograms of the wave field and a time series of the wind field going from calm to a maximum of 12 m/s during the course of the experiment. Note the strong diurnal sea breeze during much of the experiment. This is very advantageous for studying the variation of the optical transmission across the surface over a wide range of conditions.

Figure 7 shows the set up of the stereo system on the starboard boom, a pair of stereo images and the corresponding reconstruction of the surface. The stereo imagery along with the closer calibration of the scanning LIDAR permits accurate stereo imagery

reconstruction of the surface, and the wave slope statistics for input to optical transmission models.

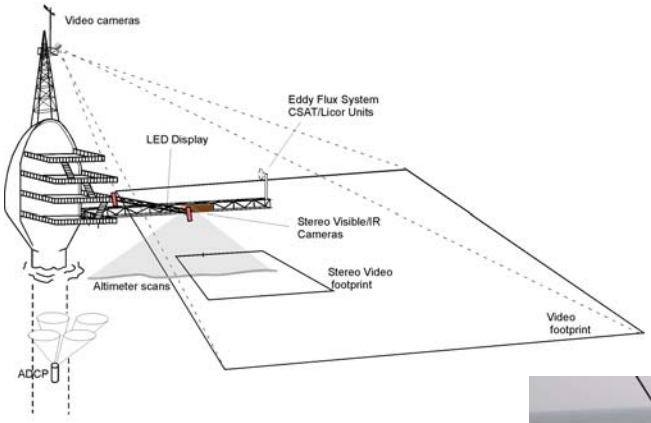

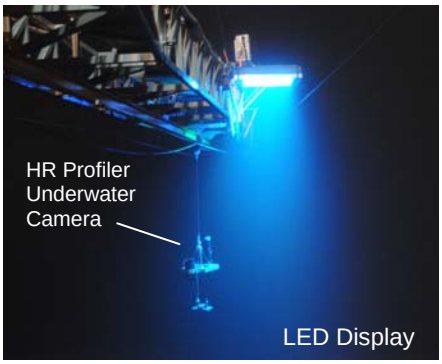

Deployed instrumentation:
11Mpx 12bit digital camera (Crow's nest)
Stereo Visible System
LED display
Dopbeam + Underwater Camera
Scanning LIDAR
Eddy Covariance system
NTP time server (GPS sync)

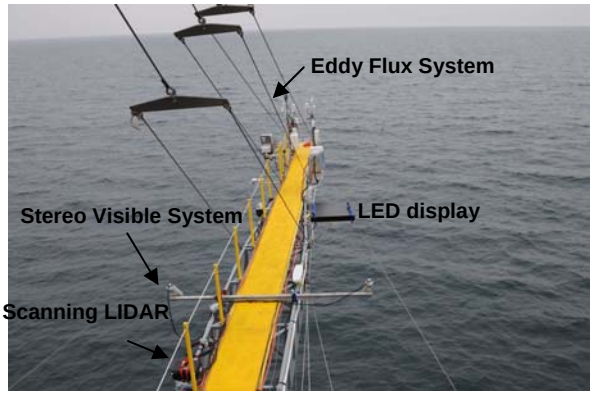

Figure 5: Deployed instrumentation during the Santa Barbara Channel Experiment in September 2008, with photographic detail of instruments on the new starboard boom.

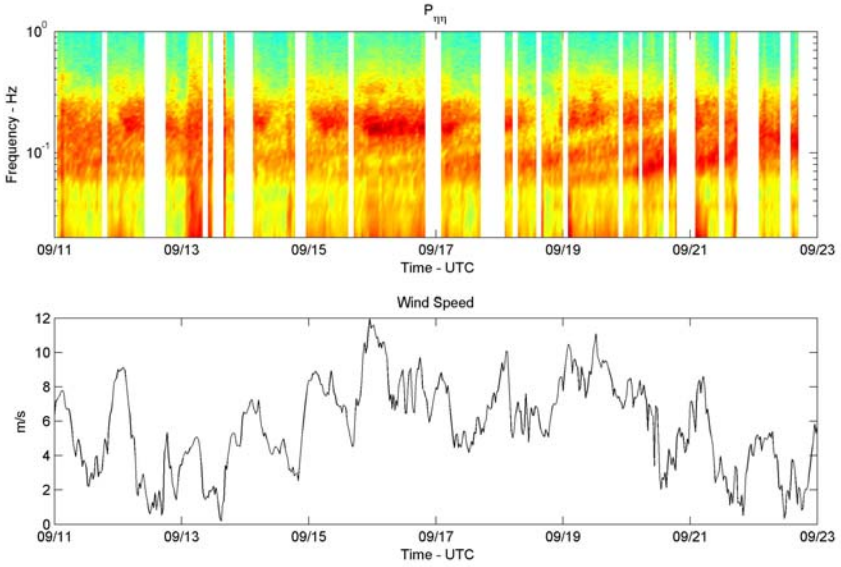

Figure 6: (Top) Surface wave displacement frequency spectrogram measured from the Scanning Laser Altimeter. Only data in the 10x10cm footprint below the instrument is considered and (bottom) wind speed measured by the ultrasonic anemometer (30min average)

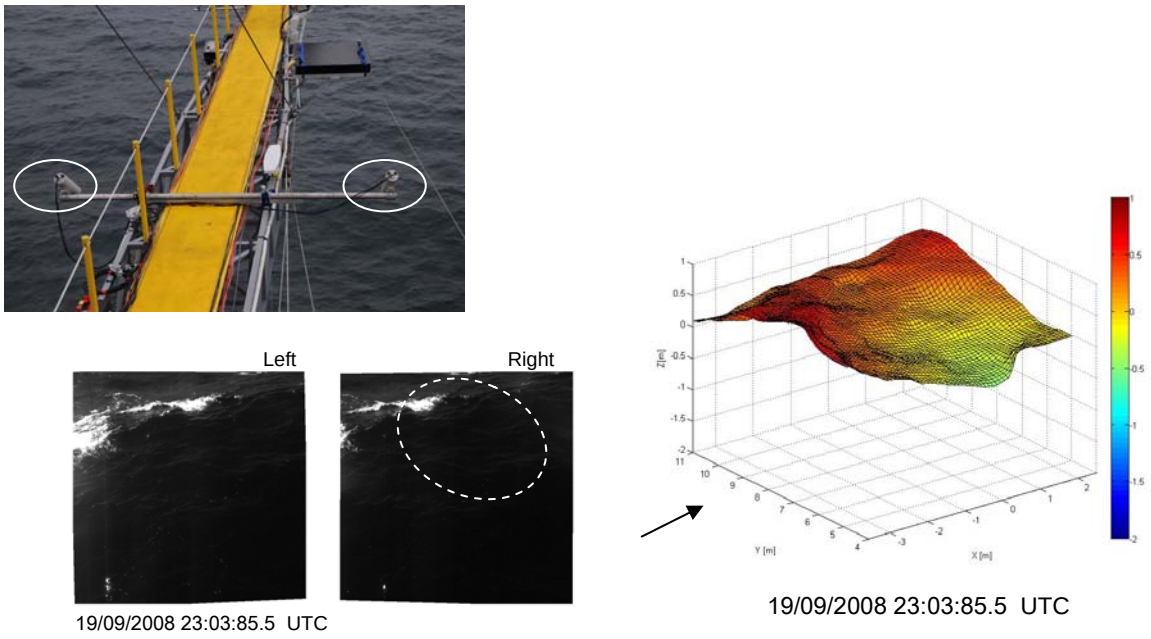

Figure 7: Stereo imagery from the starboard boom during the Santa Barbara Channel Experiment. A pair of images and its corresponding reconstruction is shown.

Hawaii Experiment August-September, 2009.

Figure 8 shows the half-hourly environmental data during the course of the experiment. They include wind speed and direction, the wind friction velocity, the significant wave height, the relative humidity and atmospheric pressure, the net radiation, the components of the radiation budget and the sensible and latent heat transfer. Note the semi-diurnal signal in the atmospheric pressure. Note the semi-diurnal tide of amplitude O(1) cm showing up in the atmospheric pressure data. The range of wind speeds, 4-12 m/s, and significant wave heights, 1.6 – 2.8 m, provides a good range of variability to investigate the variability of through-surface imaging, and environmental contributions to radiance.

Figure 9 shows acoustic Doppler measurements of the vertical velocity and backscatter from entrained bubbles.

Given that the Hawaii experiment was at the end of FY2009, more complete reporting of the results of the analysis will be contained in the FY 2010 report.

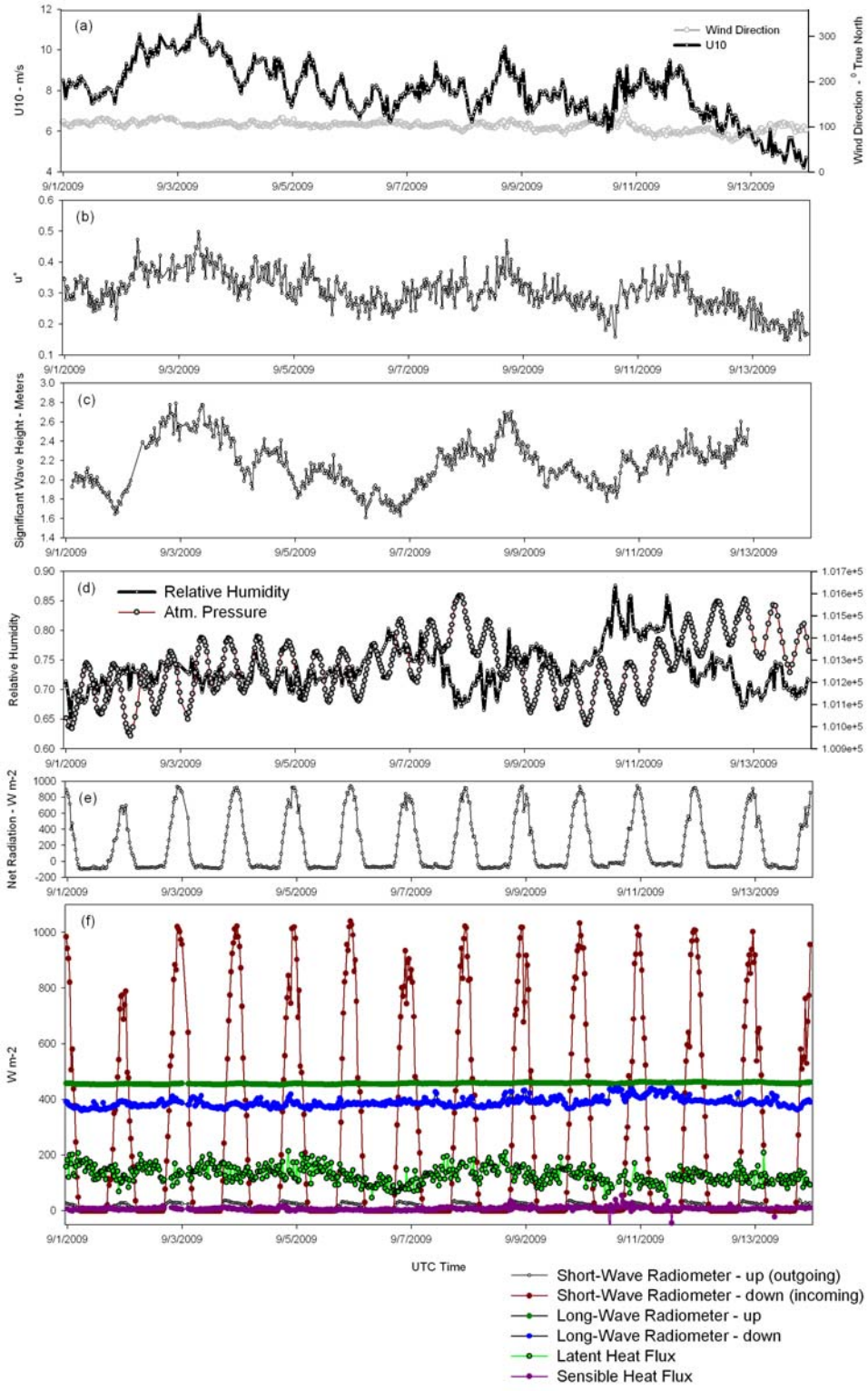

Figure 8. Preliminary environmental data during the Hawaii Experiment, September 2009.

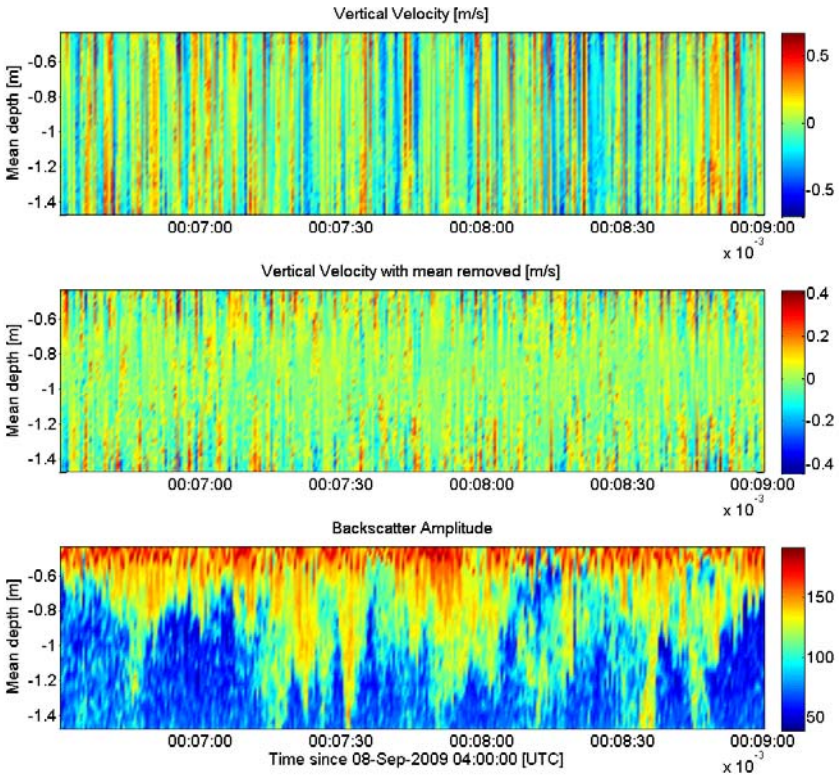

Figure 9: HR Profiler (Aquadopp) measurements of the vertical velocity and backscatter just below the surface. Top: vertical velocity showing wave background. Middle: Vertical velocity with mean over time bin removed. Bottom: Backscatter from entrained bubbles near the surface.

IMPACT/APPLICATIONS

Currently there is no impact nor applications of this work beyond the RaDyO program.

RELATED PROJECTS

Construction and testing of the new starboard and port booms and the sewage tanks was funded by a grant (and expansions) from ONR that also covered some of the logistical costs of FLIP's deployment in the Santa Barbara Channel Experiment in September, 2008. (N00014-08-1-0383, "Oceanic Radiance and Imaging: FLIP Support for September'08 Experiment")

REFERENCES

Phillips, O.M. Spectral and statistical properties of the equilibrium range in wind-generated gravity waves. *J. Fluid Mech.*,156, 505-31, 1985.

PUBLICATIONS

Reineman, BD; Lenain, L; Castel, D; Melville WK, *"A Portable Airborne Scanning LiDAR System for Ocean and Coastal Applications"*, J. Atmos. Oceanic Techn., **26**, 2626-2641, 2009.

PATENTS

None

HONORS/AWARDS/PRIZES
None